Moroccan Journal of Chemistry
ISSN : 2351-812X

Mor. J. Chem., 2023, Volume 11, Issue 02, Page 282-299
https://revues.imist.ma/index.php/morjchem

Experimental and Theoretical Evaluation of Corrosion Inhibition Performance of *Senna Obtusifolia* Leaves Extract on Mild Steel In 0.5M HCl

Abdulbasit Y.U. **(1), Abdullahi B. U. (2) and Bishir U. *(3)

[1]*Department of Chemistry, Zamfara State College of Arts and Sciences, Gusau, Nigeria.*
[2]*Department of Chemistry, Ahmadu Bello University, Zaria, Kaduna state, Nigeria.*
[3]*Department of Pure and Industrial Chemistry, Faculty of Physical Sciences, College of Natural and Pharmaceutical Sciences, Bayero Unversity, Kano. P.M.B.3011, Nigeria*
**Corresponding author, Email address: busman.chm@buk.edu.ng*
***Corresponding author, Email address: aykaura@gmail.com*

Received *18 Mar 2022,*
Revised *18 Feb 2023,*
Accepted *21 Feb 2023*

Citation*: Abdulbasit Y.U., Abdullahi B. U. and Bishir U. (2023) Experimental and Theoretical Evaluation of Corrosion Inhibition Performance of Senna Obtusifolia Leaves Extract on Mild Steel In 0.5M HCl, Mor. J. Chem., 14(2), 282-299. Doi: https://doi.org/10.48317/IMIST.PRSM/morjchem-v11i2.38203*

Abstract: Corrosion of metal is a problem which lead to serious economic lost in industries and households, and one of the most important ways to protect metallic from being destruction (corrosion) is the use of substances (inhibitor) to protect the metal corrosion. Use of green corrosion inhibitor is found to be environmentally friendly useful compare to the use of inorganic inhibitors which are toxic. Corrosion inhibition performance and adsorption effect of *Senna obtusifolia* leaves (SOL) extract on mild steel in 0.5M HCl has been assessed using weight loss measurement, potentiodynamic polarization (PDP), electrochemical impedance spectroscopy (EIS), quantum chemical analysis and molecular dynamic simulations. The inhibition performance of SOL extract was found to be 85.67% %. Similarly, the result from the PDP shows SOL extract behaves as cathodic type inhibitor also from EIS it shows increase in the concentration of the extract and charge transfer resistance with decrease in double layer capacitance from the Nyquist plot. SOL extract was found to obeys Langmuir isotherm model. Furthermore, the extract was characterized using FTIR and Uv-Visible spectroscopy which confirmed the adsorption of SOL extracts on the mild steel. SEM Surface morphology of the inhibited mild steel shows the smooth surface from assuring the protection offered by the SOL extract on the metal surface. HPLC technique suggest the main component of SOL extract responsible for the inhibition performance was found to be Kaempferol molecule at 2.99 retention time. Kinetic studies revealed that the adsorption process follows first order reaction and the half-lives of inhibited metal is greater than that of uninhibited metal The results from quantum chemical calculations confirmed good inhibition performance of SOL extract and. molecular dynamic simulation shows negative values of binding energy that is less than 100 Kcalmol^{-1} which suggests physical adsorption

Keywords: Corrosion; Inhibitor; S*enna obtusifolia*; Mild steel; Quantum Chemical Calculations

1. Introduction

Mild steel is highly ductile and wieldable. Therefore, it is used widely in industrial processing machineries and equipment in many industries including minerals, fertilizers, timber, oil, chemicals and modern semiconductor. However, the major problem associated with the use of this valuable metal is corrosion, which happens when the metal comes in contact with an acidic medium (Abdallah, 2004; Abiola, 2007). Corrosion

inhibition can be regarded as a process of donating and accepting of electrons. Whereas, the metal acts as an electrophile while the nucleophilic center is in the inhibitor (Bishir, 2015). One of the effects of corrosion is damages to oil pipelines, water pipelines, bridges, vehicles, and even home appliances (Obot *et al.,* 2011). An inhibitor retards the rate of corrosion of metals if added in minute quantity (Eddy and Odoemelam, 2009). Most inhibitors are synthesized from cheap raw materials; some are from compounds having hetero atoms (N, S, O, P) in their aromatic or long carbon chain (Adeonginyi, 2008; Eddy and Odoemelam, 2009) and also extracts of natural products (Eddy and Adeonginyi, 2010; Elmsellem *et al.,* 2014; Zerga *et al.,* 2009). Owing to the increased ecological awareness with tense environmental laws coupled with the need to develop environmentally friendly processes, attention is now focused on the development for substitute of nontoxic alternatives to inorganic inhibitors. Natural products extracted from plant sources (Bammou *et al.,* 2011; Elmsellem *et al.,* 2014), as well as some non- toxic organic compounds, which contain polar functions with nitrogen, oxygen and sulphur in conjugated systems of their molecules (Ebenso *et al.,* 2003; Ezeh *et al.,* 2023) have been effectively used as inhibitors in many corrosion systems. Previous studies have shown that ethanolic extract of *Senna Obtusifolia* leaves (SOL) contains tanins, saponinss, alkaloids, flavonoids, glycosides, (Asba and Meeta, 2017) which contains hetero atoms such as O, N, and S in their aromatic benzene rings. Therefore, it can be predicted that the adsorption of these hetero atoms on the metal surface can be used as corrosion inhibitor on mild steel in acidic medium. Many studies have been carried out on the use of various plant extract particularly leaves of different plants (Ben Hmamou *et al.,* 2012; Jimoh and Usman, 2022), however, there are a lot of promising corrosion inhibitors which are yet to be found one of the expected potential correction inhibitors is the leaves extract of (*Senna Obtusifolia*. Therefore, the aim of this research work is to investigate the inhibition performance of the leaves extract (*Senna Obtusifolia*) on mild steel in acidic medium (0.5M HCl). The structure of *Senna Obtusifolia* is presented in **Figure 1.**

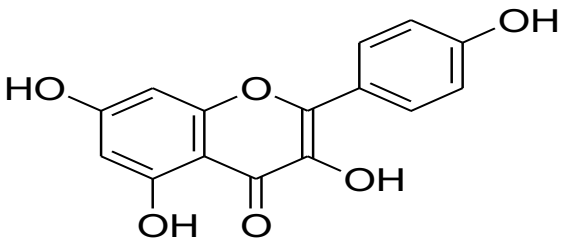

kaempferol

Figure 1: Molecular structure of Kaempferol.

2. Experimental

2.1. Preparation method of Senna obtusifolia leaves extract.2/1

The inhibitor used for this study is *Senna obtusifolia* leaves (SOL) plucked from Kaura Namoda, Zamfara sate. The leaves were taken to the Department of Plant Biology, Bayero University Kano for identification. The plant leaves were ascertained and given the Herbarium Access Number number (BUKHAN 307). The *Senna obtusifolia leaves* were shed dried, pounded into fine particles, sieved, and then sucked in a solution of ethanol for 72hrs, after which the samples were filtered. The filtrate was taken to rotary evaporator at 352K in order to make the sample free of ethanol.

2.2. Mild steel coupon preparation

Mild steel coupons were obtained from Kaura Namoda Central market and later taken to the Department of Mechanical Engineering Workshop, Bayero University Kano for confirmation. The metal sheet was pressed cut mechanically into different coupons, each of dimensions 2cm x 2cm x 2cm for weight loss and electrochemical studies. Prior to analysis, the test coupons were prepared for corrosion experiments by abrading them with different grades (600-1200) of Emery paper, then washed in ethanol, degreased in acetone, and dried in air. The coupons were then weighed and stored in a desiccator prior to corrosion analysis (Murulana, 2015).

2.3. Elemental composition of Mild steel

The mild steel was characterized using X-ray fluorescence analysis using Pal 4 Energy Dispersive X-ray Fluorescence (ED-XRF) Photometer for the identification of the elemental constituents of the metal. Mild steel pellet was loaded into the sample holder of the spectrometer; a voltage (30kV max.) and a current (1mA max.) were applied to produce X-rays which excite the metal sample for 10mins. X-ray fluorescence signals emitted all the elemental composition of the metal after the photoelectric ionization which are measured simultaneously in a fixed mounted semiconductor detector. The concentration of the elements in the sample which is proportional to the radiation intensity of each element signals, were calculated internally from a stored set of calibration curves.

2.4. Weight loss

This was carried out in accordance with the ASTMG 1-03 standard procedure. To obtain the Weight loss, the weight of the metal obtained before and after the weight loss. The test was carried out in a conical flask with 100ml of 0.5M HCl. The samples were dipped in the flask for about 5hrs with varying temperatures, viz., 30-60^{0}C. After immersion time, the samples were retrieved, washed with distilled water and subjected to oven for 10mins. After obtaining the results, it was which was used to calculate the corrosion rate, surface coverage, and inhibitor efficiency using equations 1, 2, and 3 respectively.

$$CR = \frac{gh/h}{cm^2} = \frac{\Delta w}{At} \quad (1)$$

$$\theta = 1 - \frac{w^1}{w^2} \quad (2)$$

$$\%I = \left(1 - \frac{w^1}{w^2}\right) \quad (3)$$

Where w_1 and w_2 are the weight losses (in g) for mild steel coupons in the presence and absence of the inhibitor in HCl solutions respectively. ɵ is the degree of surface coverage of the inhibitor, A is the area of the metal coupon (cm^2), t is the immersion time (hrs) and Δw is the weight loss of mild steel coupon (g) after time (t) (Omotosho, 2016)

2.5. Potantiodynamic dynamic polarization (PDP)

The electrochemical measurements were performed in a three-compartment glass cell consisted of the mild steel specimen as working electrode (WE), platinum counter electrode (CE), and a saturated calomel electrode (SCE) as the reference electrode. The counter electrode was separated from the working electrode compartment by glass. The reference electrode was connected to a Luggin capillary to minimize IR drop. Solutions were prepared from distilled water of resistivity 13 MX cm. The electrode potential was allowed to stabilize 60 min before starting the measurements. All experiments were conducted at 30^{0}C. Measurements were performed using Gamry Instrument Potentiostat/Galvanostat/ZRA. This includes a Gamry Framework system based on the ESA400, Gamry applications that include dc 105 for dc corrosion measurements, Echem Analyst 5.58 software was used for plotting, and graphing and fitting data Tafel polarization curves were obtained by changing the electrode potential automatically at open circuit potential with scan rate of 1.0 mVs. Corrosion current density (*Icorr*) and corrosion potential (E_{corr}) were obtained and the inhibition efficiency (μ_p) at varying inhibitor concentrations was calculated using equation 4:

$$\mu_{p\ (\%)} = \frac{i^o_{corr} - i^i_{corr}}{i^o_{corr}} \text{ x100} \quad (4)$$

Where I^0_{corr} and I^i_{corr} are the corrosion current density in the absence and presence of the extracts respectively. Inhibition efficiency from the polarization resistance (Rp) was determined using equation 5.

$$\mu_{PR}\ (\%) = \frac{R^i_p - R^o_p}{R^i_p} \text{ x100} \quad (5)$$

R^i_p and R^0_p donates linear polarization resistance in the presence and absence of the inhibitor respectively.

2.6 Electrochemical Impedance Spectroscopy (EIS)

Measurements were performed using Gamry Instrument Potentiostat/Galvanostat/ZRA. This includes a Gamry Framework system based on the ESA400, Gamry applications that include dc105 for dc corrosion measurements, EIS300 for electrochemical impedance spectroscopy measurements along with a computer for collecting data. Impedance measurements were carried out in frequency range from 10 kHz to 10.0 mHz with an amplitude of 10mV peak-to-peak using ac signals at open circuit potential. The inhibition efficiency (μ_{Rt}) was calculated for each inhibitor concentration using equation 6.

$$\mu_{Rt}\ (\%) = \frac{R_t^i - R_t^o}{R_t^i}\ \text{x}100 \qquad (6)$$

Where R^i_t and R^0_t indicates charge transfer resistance without and with various concentrations of the inhibitor respectively. The double layer capacitance was determined using equation 7.

$$C_{dl} = \frac{1}{2\Pi f_{max} R_t} \qquad (7)$$

Where f_{max} is the maximum frequency. Rt is the charge resistance.

2.7 High performance liquid chromatography (HPLC)

The chromatogram of the extract was carried out using HPLC. *Senna obtusifolia* leaves (SOL) were been dried, pounded to powder, sieved, and soaked in ethanol for 72 hrs to form an extract, after which the samples were filtered and subjected to rotary evaporator in order to leave the sample free of the ethanol extract ready for HPLC analysis. The concentrate was then dissolved in 10ml of methanol (HPLC grade). Chromatographic analysis was carried out using a column, C-18 at 38^0C. This was equilibrated with the corresponding mobile phase (acetonitrale) and stationary phase in ratio of 80:20; flow rate at 0.15mL/min; running time of 20 mins; and UV detection at 254nm. 30 µL of the extract was filtered with PTFE syringe (0.43nm), Whatman (U.K). A 10 µL of the extract was injected through a syringe in HPLC for instrumentation. The compounds in the extract were identified by comparison with their retention time with the retention time of standard pure compounds in order to identify the main chemical constituent of the *Senna Obtusifolia* leaves (SOL) (Prakash *et al*, 2015).

2.8 UV-Visible Spectroscopy

Perkin Elmer UV WinLab Data Processor and Viewer Version 1.0, UV/Vis Spec instrument was used to carried out the optical characterization of the extract in the absence and the presence of the inhibitor to observe if the inhibitor is adsorbed on the surface of the coupons. 0.8g/l of the samples were checked at the wavelength range of 200-900nm. After 2hrs, samples were gained, washed with distilled water and cleaned three times before immersing in distilled water for 30mins. Then finally, smooth rubbing of the sample surfaces, these solutions were been examined again and compared with pure extracts of the plant in order to observe if there are any significant changes (Onen, 2010)

2.9 Fourier Transform Infrared Spectroscopy (FTIR)

Two coupons were separately dipped in 100ml of 0.8g/l inhibitor concentration for 48hrs in order to form adsorbed layer after which they were retrieved, dried, corrosion products were obtained and FTIR

was used to analysis and observed the changes. The samples were prepared using KBr plate and done by scanning the sample through a wave number range of 400-4000cm^{-1} (Murulana, 2015).

2.10 Surface Analysis

The micrograph of mild steel coupon subjected to solution with and without inhibitor was analyzed using Scanning Electron Microscopy (SEM analysis). An S50 Scanning Electron Microscope was used to study the surface morphology of the fresh mild steel in solution of 0.5M HCl and inhibitor of 0.8g/L. The coupons were dipped in blank solution and 0.8g/L of the inhibitor. The coupons were then retrieved, rinsed with distilled water, and dried. The coupons were mounted on a metal stub and sputtered with gold in order to make the coupons conductive (Kalaichelvi and Dhiyya, 2017).

2.11 Quantum chemical Details

Density Functional Theory (DFT) is considered to study the inhibitor interaction. This is also considered as a unique approach to study the reaction mechanism in the field of corrosion reaction mechanism (Usman, *et al.,* 2018). The quantum chemical calculations were carried out with Material Studio (version 8.0). Molecules optimization was carried using DFT at Becke three Yarg and Parr with 6-311G++ (d,p) basis as B3LYP/6-311G++ (d,p) using Spatan 14. The quantum chemical assessments were used to search for good quantum chemical descriptors to explain the inhibitive performance of the molecule. The molecular descriptors such as electronegativity (X), ionization energy (I), electron affinity (A), hardness (η), softness (S), fractions of electrons (ΔN), global electrophilicity index (φ), and Back donation energy change (ΔE_{BD}) were calculated using equation 8-16.

$$A = -E_{LUMO} \quad (9)$$

$$\Delta E_{gab} = -E_{LUMO} - E_{HUMO} \quad (10)$$

$$\chi = \frac{I+2}{2} \quad (11)$$

$$\eta = \frac{I+2}{2} \quad (12)$$

$$S = \frac{I}{\eta} = \frac{2}{I-A} \quad (13)$$

$$\Delta N = \frac{X_{Fe} - X_{inh}}{[2(\eta_{Fe}) + \eta_{inh}]} \quad (14)$$

$$\varphi = \frac{X_{inh}^2}{4\eta} \quad (15)$$

$$\Delta E_{BD} = -\frac{\eta}{4} \quad (16)$$

Where X_{Fe} and X_{inh} Are the absolute electronegativity of iron and inhibitor respectively, η_{Fe} *and* η_{inh} indicates the absolute hardness of iron and inhibitor respectively. A theoretical value of 7eV is for iron, and η_{Fe}= 0 is assumed that I = A for bulk metals, because they are softer than the neutral metallic atoms. This method was found to be used (Usman, *et al.,* 2018).

2.12 Molecular Dynamic Simulation

Molecular dynamics (MD) simulation was carried out using Materials Studio (version 8.0). Fe was the chosen surface for this simulation study. Fe was first cleaved along the (110) plane with the uppermost and lowest layers fixed. A simulation cubic box (12.5 Å × 12.5 Å × 12.5 Å) with fixed Number-Volume-Energy (NVE) (microcanonical) ensemble was used for the execution of the molecular dynamic simulation of the interaction between Kaempferol molecule and Fe (110) surface. The optimization of the iron with (110) plane was first computed to minimum energy, followed by addition of the inhibitor molecule next to the surface and the behavior of the molecule on the Fe (110) surface was simulated using compass force field (version 2.8). The MD simulation was performed

under 298 K, NVE ensemble, with a time step of 1fs and simulation time of 5ps (Umar, *et al.,* 2019). The binding energy (E_{bind}) and the interaction energy between the iron surface and the inhibitor molecules was calculated using equations 18 and 17 respectively.

$$E_{Interaction} = E_{total-}(E_{Fe} + E_{inh}) \quad (18)$$

Where E_{Total} is the total energy of iron crystal together with the adsorbed Kaempferol molecule, E_{Inh} and E_{Fe} are the energy of free Kaempferol molecule and Iron crystal respectively. The binding energy of the inhibitor molecule is the negative value of the interaction energy and is given by equation17:

$$E_{Interaction} = -E_{Binding} \quad (17)$$

Therefore, E_{Bind} is the Negative value of $E_{Interaction}$ (Kalaichelvi & Dhiyya, 2017; Usman, *et al.,* 2018)

3. Results and Discussion

3.1 Elemental composition of metal

The results of metal characterization were carried out using XRF which revealed the types of metal as mild steel, presented in **Table 1** represents the elemental composition of mild steel coupon, it was found to 0.066% carbon which is within the range (0.05-25%) maximum of carbon content for mild steel in accordance with ASTM standard guidelines. These findings confirms that the metal sample used was mild steel

Table 1: Elemental Composition of Mild Steel Coupon (%wt)

Elements	Composition (%wt)
C	0.066
Si	0.130
Al	0.040
Ca	0.010
Mn	0.270
Cr	0.041
Cu	0.023
Te	0.170
I	0.250
Cl	0.210
Sc	0.030
Sb	0.200
Eu	0.100
Fe	98

3.2 Characterization of Senna obtusifolia leaves extract.

3.3 HPLC analysis

The HPLC was used to identify the main constituent of the SOL leaves extract responsible for the corrosion inhibition. From the chromatogram in **Figure 2**, the major component appeared at retention time of 2.990min. The molecule was found to be Kaempferol by retention time (2.990min). Therefore, Kaempferol molecule (flavonoid family) was found to be the main constituent of ethanolic extract of SOL (Doughari *et al.*, 2008; Jan and Patil, 2010)

3.4 UV- Vis spectroscopy

Figure 3 illustrates the UV-Vis spectra for SOL extreact and SOL extract adsorbed on mild steel surface respectively. Careful investigation of spectra A shows peak appearance between 204.04nm-673.72nm with absorbance of 1.62A and 0.29A respectively in the spectral of the extract which the supported the presence of saponins, tannins, alkaloids, flavonoids, steroids, phenols, and glycosides among others. The results from spectra B shows change in wavelength (262.89-674.51nm) and absorbance (0.41A and 0.11A respectively) due to corrosion inhibition performance of the inhibitor on mild steel. The findings indicates adsorption of bioactive compounds present in the SOL extracts (Prakash *et al*, 2015; Kalaichelvi and Dhiyya, 2017).

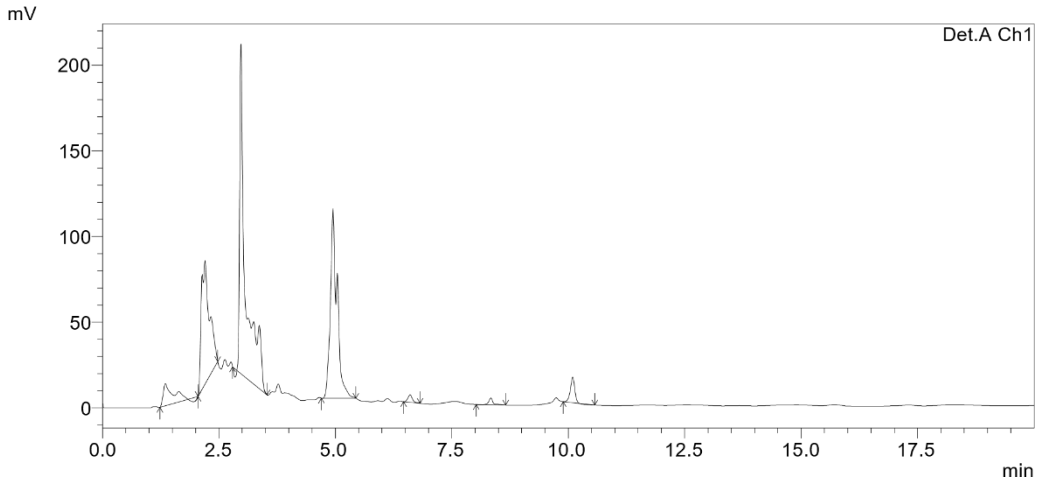

Figure 2: HPLC Chromatogram of Ethanolic Exract of *Senna obtusifolia*

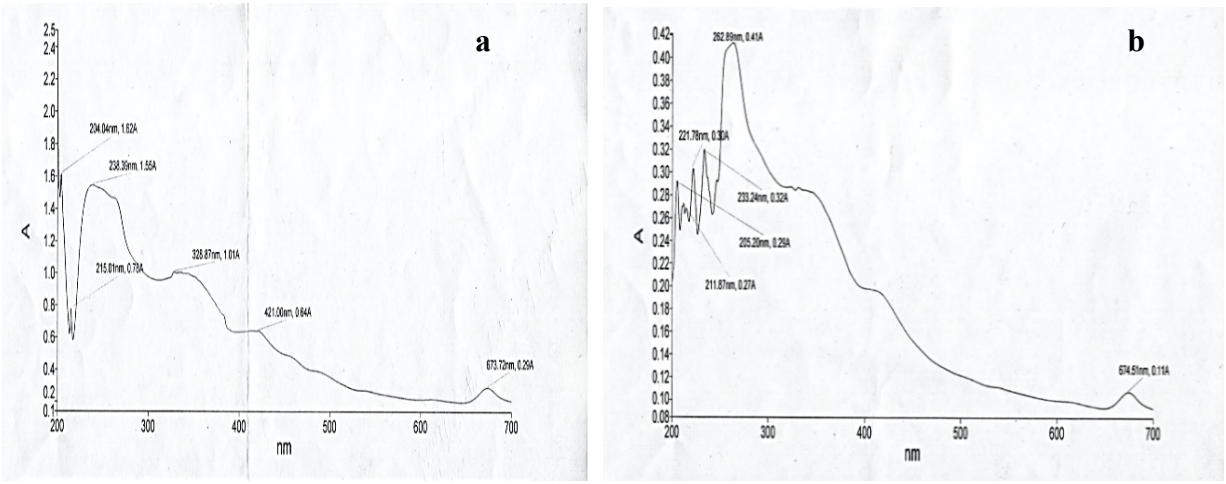

Figure 3: UV Visible Spectra of **(a)** *Senna obtusifolia* Leaves Extract and **(b)** *Senna obtusifolia* Leaves Extract Adsorbed on Mild Steel Surface. The HPLC chromatogram showing the highest peak around 250mv indicating Kaempferol

3.5 FTIR analysis

IR spectra of the SOL extracts and the corrosion product when SOL extract was used as an inhibitor is shown in **Figure 4**, which shows peaks with different intensities. From the results obtained in **Figure 4**, it shows that, C-H stretch at 2925cm^{-1} and 2854cm^{-1} was shifted to 2921cm^{-1} and 2851cm^{-1} respectively. The O-H stretch at 3279cm^{-1} was shifted to 3305cm^{-1}; C=C stretch at 1611cm^{-1} was shifted to 1622cm^{-1}; C-H saturated at 2095cm^{-1} was shifted 2084cm^{-1}. These shifts in frequencies

indicated that, there was interaction between the inhibitor and the metal surface. It also shows from the **Figure 3**, that a shift occurred in CH_2 bend, CH_3 bend, and N=O showing an interaction between the metal surface and SOL extract (Prakash *et al.*, 2015; Kalaichelvi and Dhiyya, 2017; Boudalia, *et al.,*2013), which confirmed the corrosion inhibition took place.

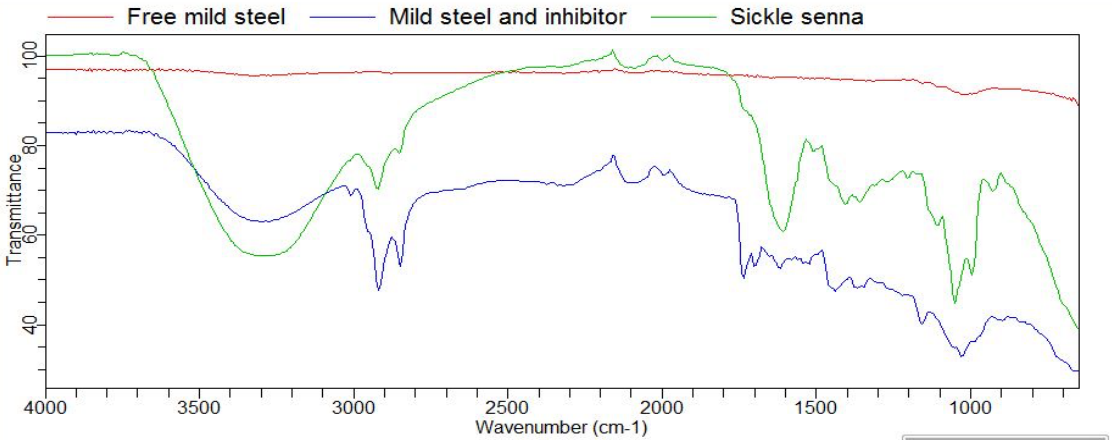

Figure 4: Overlay for FTIR Spectra of Free Mild Steel, Mild Steel and Inhibitor, and *Senna obtusifolia* Leaves. The spectrum **(a)** is the free metal spectra, while extract is presented in **(b)** spectrum **(c)** indicate the corrosion inhibition process of the extract on the metal surface showing appearance and disappearance of peaks

3.6 SEM analysis

The SEM micrographs for different coupons of mild steel in the presence and absence of SOL extract are shown in **Figure 5**. **Figure 5a** indicates fresh mild steel which has a smooth surface; while **Figure 5b**, indicate the micrograph for the corroded mild steel which has cocoon like structure showing the damage surface of the mild steel. From **Figure 5c** micrograph, it shows an improved smooth surface morphology indicating the presence of SOL extract absorbed on the surface of the mild steel. This change in surface morphology confirmed the protection offered by the extract on the surface of the mild steel immersed in the acid medium (Boudalia *et al.,* 2013 ; Prakash *et al.*, 2015).

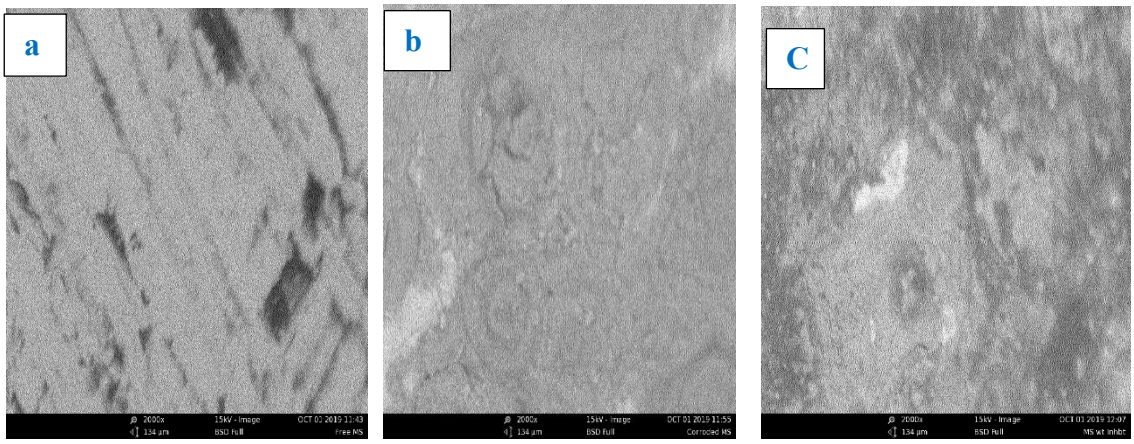

Figure 5: SEM Micrographs of Mild Steel: **(a)** Fresh Mild Steel, **(b)** Corroded Mild Steel, and **(c)** Mild Steel with Inhibitor. The micrographs **(a)** represent the surface of metal without any treatment showing a smooth surface while **(b)** indicate the destruction of the surface in acidic media while **(c)** revealed how effectiveness of the extract as corrosion inhibitor due the smoothness of surface

3.7 Weight loss measurements

3.8 Effect of Temperature on Corrosion Rate

Temperature effect was assessed using weight loss analysis on mild steel in 0.5M HCl solution with varying concentrations of SOL extracts at different temperature ranges. **Figure 7** shows as the temperature of the system

is increased, the corrosion rate also increases due to the increased in kinetic energy of the reacting molecules. This shows that, SOL extract is an inhibitor of mild steel corrosion in 0.5M HCl solution (Du *et al.,* 2014).

3.9 Effect of Inhibitor Concentration

Figure 6 illustrates the effect of SOL extract concentration on corrosion rate and inhibition efficiency at different temperature range for mild steel in 0.5M HCl respectively. It's evident from **Figures 6-7,** that the corrosion rate has a direct proportionality with the temperature as well as the concentration of the extract. **Figures 8-9** shows an increased inhibition efficiency accompanied by SOL extracts but reduces with higher temperature due to increase in kinetic energy. This finding shows that, the SOL extract has good inhibition efficiency potential in acidic medium (0.5M HCl) (Du *et al.,* 2014; Omotosho, 2016).

3.10 Effect of Temperature on Inhibition Efficiency

Relationship between temperature and inhibition efficiency has been found to be an inverse relationship from **Figure 8,** shows that as the temperature goes up, the inhibition efficiency goes down. The increase and decrease was mainly due to the change in kinetic energy of the reacting molecules. This findings are in mutual agreement with that of (Eddy *et al.,* 2008; Onen, 2010)**.**

3.11 Effect of Immersion Time

The findings for the effect of immersion time on corrosion rate of mild steel in 0.5M HCl in the presence and absence of SOL extract is shown in **Figure 10-11.** It is clear there is rapid increase of weight loss with increasing contact level. But the effect was reversed as the concentration of SOL extract is increased. This result clearly shown that as the SOL extract is increased, the low weight of the mild steel decreased, forming a protective layer within 24hrs of contact time.

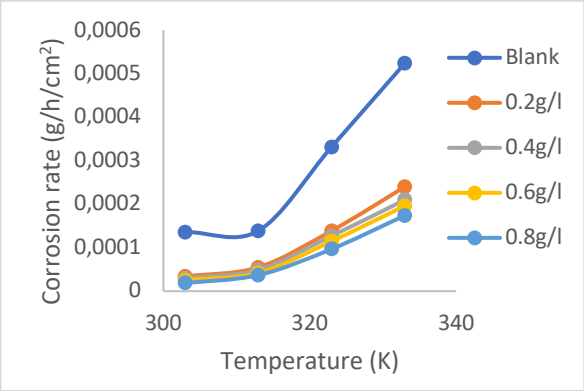

Figure 7: Corrosion Rate of Mild Steel against Temperature (303K-333K) in the Absence and Presence of SOL Extract in 0.5MHCl.

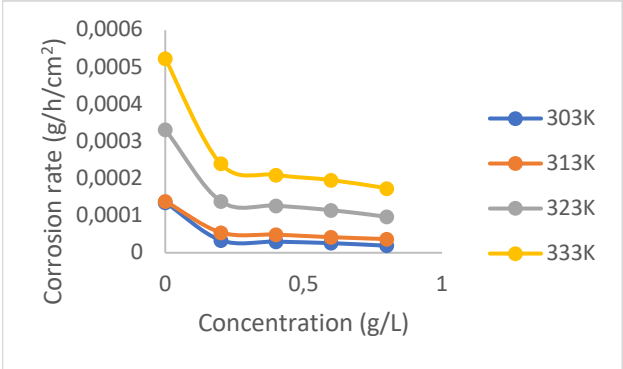

Figure 6: Corrosion Rate of Mild Steel against Various Concentration of SOL Extracts in 0.5M HCl at 303K-333K..

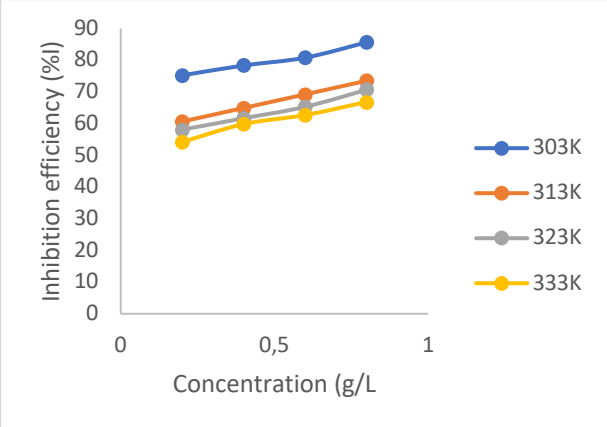

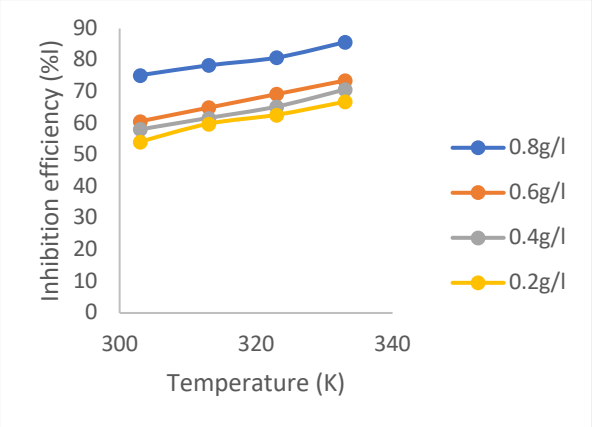

Figure 9: Inhibition Efficiency (%*IE*) against Temperature for the Corrosion of Mild Steel in 0.5M HCl

Figure 8. Inhibition Efficiency (%*IE*) against Concentration of the SOL Extract for Mild Steel in 0.5M HCl at 303K-333K

The property of the inhibition efficiency by the SOL extract was due to its ability to be adsorbed on the steel surface and formed a protective layer. This protective layer the metal surface from the corrosive environment. This finding conforms to that of (Eddy *et al.,* 2008; Du *et al.,* 2014; Omotosho, 2016; Khadim, 2016). The plots from **Figs. 10 -11** show that, at 303K the SOL extract retained more than 80% of its inhibition potential even after 7days (168hrs) immersion time. This results were in agreement (Omotosho, 2016; Jimoh and Usman, 2021).

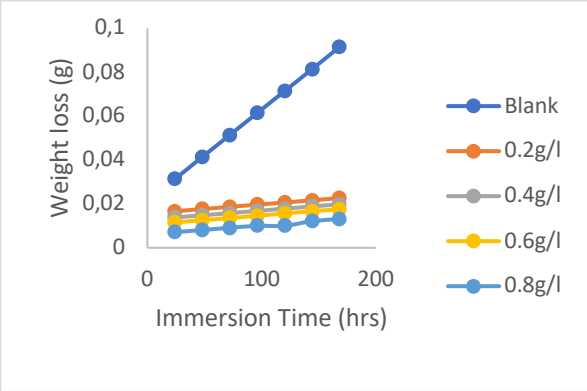

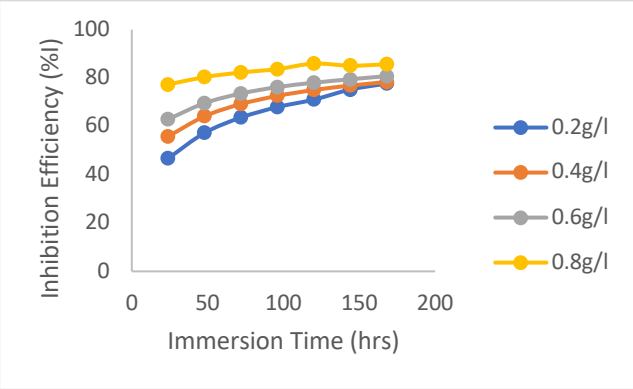

Figure 10: Effect of Immersion Time on Corrosion Rate of Mild Steel in 0.5M HCl in the Presence and Absence of the SOL Extract at 303K

Figure 11: Effect of Immersion Time on Inhibition Efficiency of the SOL Extract on the Dissolution of Mild Steel in 0.5M HCl at 303K.

3.12 Adsorption Isotherms

The values for the intercepts, slopes, R^2, and K_{ads} parameters for Langmuir adsorption isotherm for the adsorption of SOL extract on mild steel surface at different temperature (303K-333K) are presented in **Table 2**. These values (intercepts, slopes, R^2, and K_{ads}) were obtained from **Figure 12**, higher adsorption effect is as a result of different concentration many constituents of the extract.

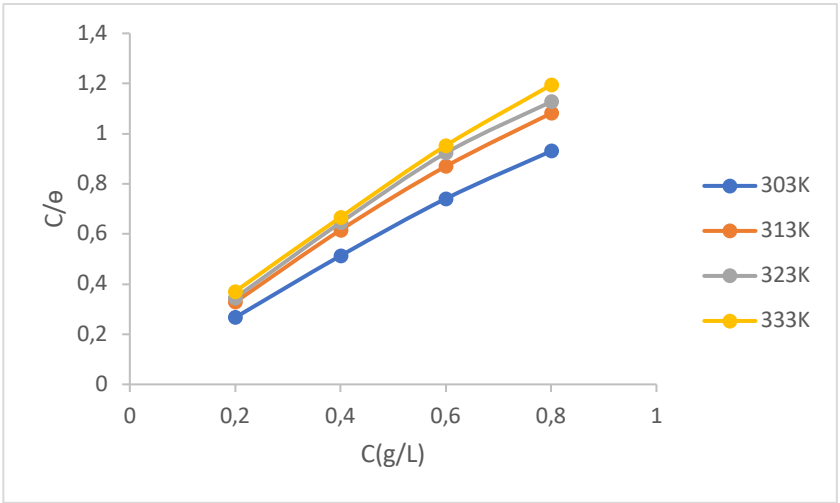

Figure 12: Langmuir Isotherm for the Adsorption of SOL Extract on Mild Steel in 0.5M HCl at 303K- 333K

Table 2: Langmuir Adsorption Isotherm for the Adsorption of SOL extract on Mild Steel Surface at 303-333K

Temp.	Intercept	Slope	K_{ads}	R^2
303K	0.0581	1.092	17.2117	0.9967
313K	0.0951	1.2569	10.5152	0.9954

323K	0.1040	1.3120	9.6154	0.9929
333K	0.1067	1.3784	9.3721	0.9909

3.13 Potantiodynamic polarization study

The results from Tafel polarization curve were confirmed and presented in **Figure 13**. The results shows that SOL extract is a cathodic type inhibitor. From the analysis, it was revealed that equilibrium potential (E_{corr}) changes and corrosion current density (I_{corr}) goes down with inhibitor concentration, which elucidated that the organic constituents of the extracts inhibited the corrosion rate of mild steel in HCl solutions. The corrosion parameters which were computed from Tafel polarization curves are listed in **Table 3**. A careful investigation of Tafel parameters elucidated that addition of inhibitor displaced E_{corr} of corrosion reactions, but displacement of E_{corr} values did not indicate any pattern. This conforms the findings of Li *et al.,* (2008). The magnitude of b_a and b_c also changed with inhibitor concentration; however, the shift was found to be mix inhibitor. This fact supported the changes that occurred in E_{corr} values on addition of the inhibitor. Furthermore, it was noticed from the **Table 2** that, I_{corr} values decreased with increased in inhibitor concentration indicating that the extracts retarded the corrosion rate of mild steel samples in HCl solution. This shows that, the SOL extract is active corrosion inhibitor. This was in agreement to the polarization resistance which increased with extracts concentration (Du, 2014)**.**

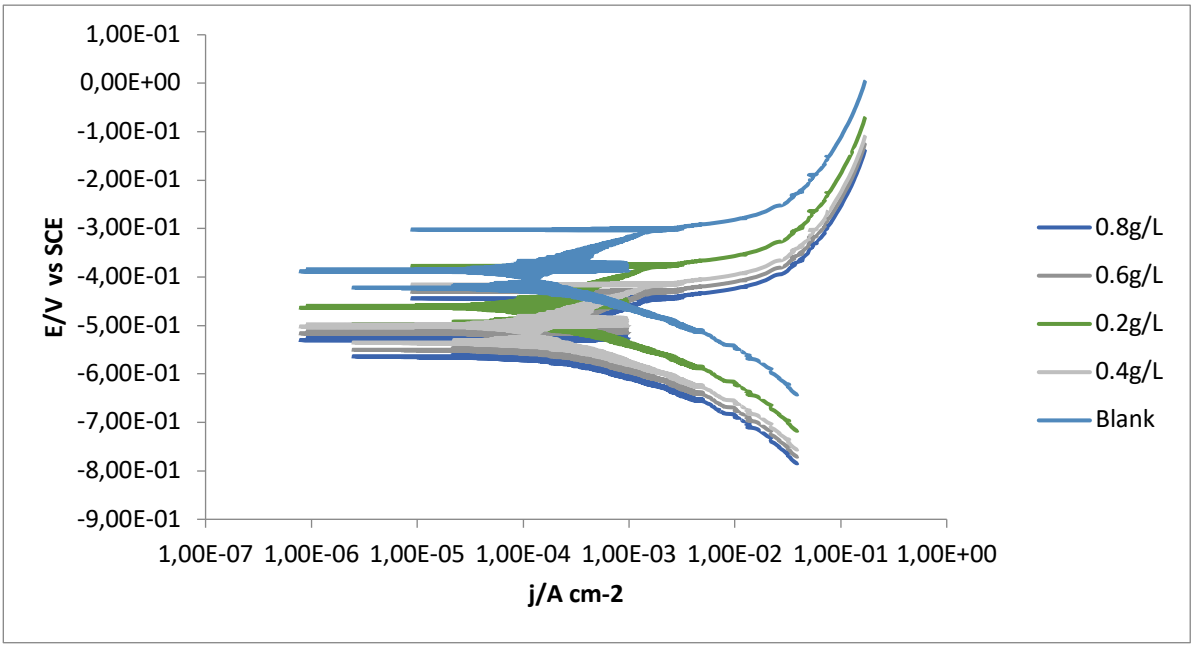

Figure 13: Tafel Polarization Curves for Mild Steel with Different Concentrations of SOL Extract in 0.5M HCl.

Table 3: Tafel Polarization Parameters at Different Conc. Of SOL extract for Mild Steel in 0.5M HCl.

Conc. (g/L)	$-E_{corr}$ (mV)	I_{corr} x 10^{-5} (A/cm^2)	ba (mV/dec.)	-bc (mV/dec.)	CR ($mmyr^{-}$)	µP (%)	Rp (Ωcm^2)	µPR%
Blank	584.61	49.20	3.96	7.28	3.54	-	31.27	-
0.2	534.81	18.25	3.89	7.76	2.19	62.90	78.69	60.26
0.4	554.68	16.12	3.76	7.62	1.74	67.24	89.86	65.20
0.6	499.00	13.80	3.62	7.89	1.59	71.95	107.10	70.80
0.8	497.08	10.81	3.20	7.20	1.49	78.03	127.90	75.55

3.14 Electrochemical impedance spectroscopy

Nyquist plots of mild steel in 0.5M HCl solution in the presence and absence of SOL extract at 300C is presented in **Figure.14**. The shape of the Nyquist diagram provides information on the electrode interface between the metal surface (Du, 2014)**.** It is evident from **Figure14,** the electrochemical response decreased semicircles, indicates a capacitive layer was formed at metal acid interface. The loops diameters seemed to

increase with increased SOL extracts concentration pointing that, charge transfer process at the interface reversed due to the presence of the SOL extracts. The technical details of the impedance spectra were investigated using an equivalent electrochemical circuit shown in **Figure 15** contained various parameters such as solution resistance (Rs), charge resistance (Rt), and double layer capacitance (C_{dl}). From **Table 4**, it is revealed that, Rt values increase with increased SOL concentrations while C_{dl} decreased. An increased in R_t values could be ascribed to the molecular adsorption of the extract on metal acid interface, which effectively blocked the movement of changes across the interface and hence corrosion inhibition acknowledged. This is due to the decreased in C_{dl} values (Du, 2014; Ghazoui et al. 2017)**.**

Table 4. Technical Parameters Obtained from Nyquist Plots at Different Conc. Of SOL extract for Mild Steel in 0.5M HCl.

Conc. (g/L)	Rs (Ωcm^2)	Rt(Ωcm^2)	C_{dl}($mFcm^{-2}$)	μ_{Rt} %
Blank	0.20	29.67	53.59	-
0.2	1.61	77.09	20.60	61.51
0.4	0.91	88.26	14.32	66.38
0.6	0.96	105.48	9.519	71.87
0.8	1.46	125.28	6.360	76.32

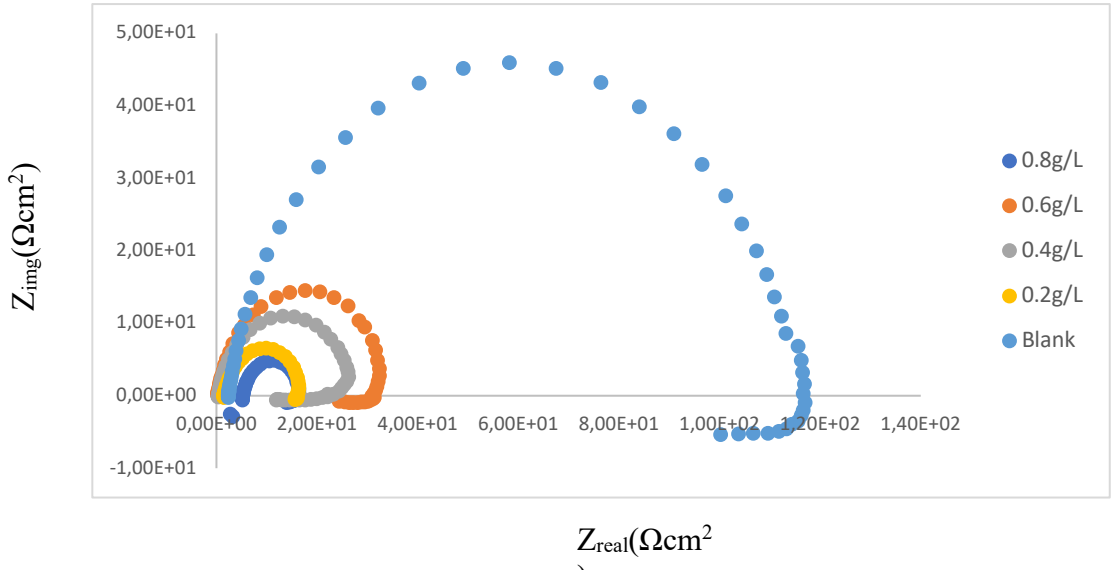

Figure 14: Nyquist Plots for Mild Steel in the Absence and Presence of Various SOL Extract Concentration in 0.5M HCl.

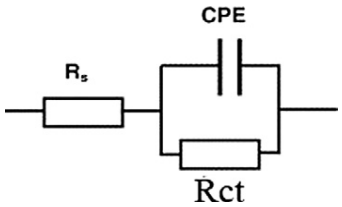

Figure 15: Electrochemical Circuit

3.15 Quantum chemical calculation

Quantum chemical calculation was carried out in order to investigate the effect of molecular structure on corrosion behavior of SOL extract with quantum chemical descriptors to support the result**.** **Figure 16** represents the optimized structure of E_{HOMO}, and E_{LUMO} of Kaempferol molecule. The quantum chemical descriptors were calculated and presented in Table 5. Results show the values of E_{HOMO}, E_{LUMO}, and ΔE_{gap} describe the ability of the compounds to donate and accept electron from the metal d-orbital. Therefore, higher value of E_{HOMO} with lower value of E_{LUMO} and ΔE_{gap} the better the release and acceptance of electron by Kaempferol molecule. Henceforth, the E_{HOMO} (-5.534eV), E_{LUMO} (-1.81eV), and ΔE_{gap} (7.34eV) gives a good inhibition efficiency. This conforms to findings of (Umar *et al.,* 2019). According to (Umoren *et al.,* 2012; Usman *et al.,* 2015), η and S

measured the stability of molecules and hard molecules have higher ΔE_{gap} while soft molecules have smaller ΔE_{gap}, and molecules with lower η values and higher values of S tends to give good corrosion inhibition efficiency (Usman *et al.,* 2015), reported that lower values of A, I, and higher χ and TE gives better inhibition efficiency. Similarly, the values of χ (3.67eV), I (5.53eV), A (1.81eV), S (0.54eV), and η (1.86 eV) give the SOL extract to be a good corrosion inhibitor [4], reported that, there is no relationship between dipole moment (μ) with the inhibition efficiency (%IE) experimental (Du, 2014) found that, an electronic back-donation (ΔE_{BD}) process might be occurring due to interaction between the inhibitor molecule and the metal surface. The ΔE_{BD} implies that when $\eta > 0$ and $\Delta E_{BD} < 0$, the charge transfer to a molecule followed by ΔE_{BD} from molecule, will be favored energetically. From table 4, η=1.86ev and ΔE_{BD} = -0.47eV shows that the back-donation from the molecule was favored energetically and has an inverse relation to hardness. This conforms to the findings (Usman *et al.,* 2015).

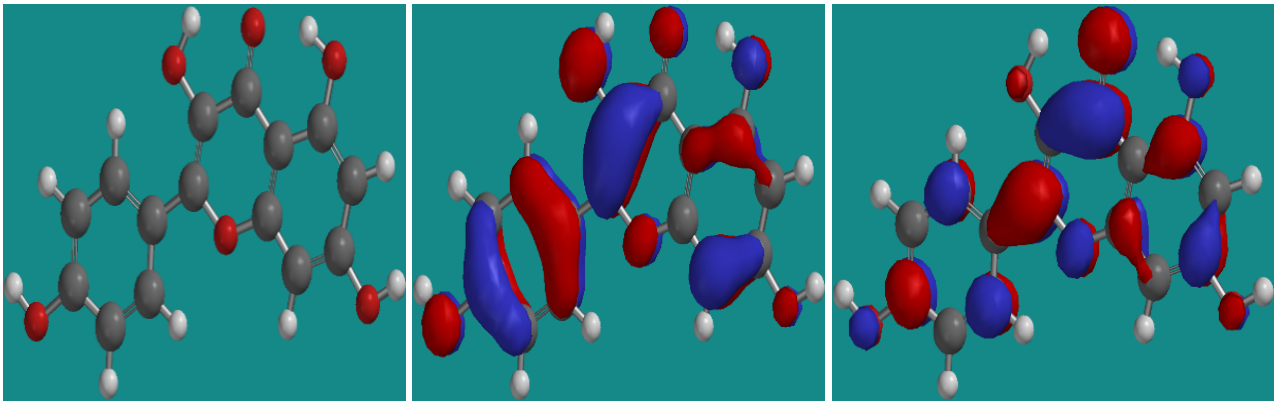

Figure 16: Optimized Structure, E_{HOMO}, and E_{LUMO} of Kaempferol

Table 5: Quantum Chemical Descriptors and their Value

Descriptors	Values
E_{HOMO} (eV)	-5.53
E_{LUMO} (eV)	-1.81
ΔE_{gap}(eV)	7.34
χ (eV)	3.67
I (eV)	5.53
A (eV)	1.81
S (eV)	0.54
η (eV)	1.86
μ (debye)	1.54
Δ*N* (eV)	0.90
φ(eV)	1.81
ΔE_{BD} (eV)	-0.47
TE	-120.03

The inhibition effect resulting from electron(s) donation was represented by the symbol (ΔN). The inhibition efficiency increases by increasing electron donating ability of the inhibitor to donate electrons to the metal surface if ΔN < 3.6 eV (Usman *et al.,* 2015), From the table 4, ΔN = 0.90 eV shows that the inhibition efficiency resulting from electron donation agrees with (Usman *et al.,* 2015), study and correlates with the experimental inhibition efficiency strongly. Also, the positive value of ΔN shows that, the molecule acts as an electron donor in aqueous medium. This correlates to the findings (Eddy *et al.,* 2008; Du *et al.,* 2014; Usman *et al.,* 2015),

reported that, the higher the value of φ, the higher the capacity of the molecule to accept electrons. From Table 4, φ = 1.81 eV, showing that the Kaempferol has lower capacity to accept electrons, the total energy (TE) of the inhibitor molecule (Kaempferol) is -1021eV, which shows that the inhibitor molecule (Kaempferol) is favorably adsorbed through active centers on the mild steel (Abuabakar and Usman, 2019; El Ghayati *et al.,* 2019; Alhassan and Usman, 2019; Ibrahim *et al.,* 2019; Husaini, et al.,20193a; Husaini, *et al.,*2019b; Khaled, 2010).

3.16 Molecular dynamic simulation

The adsorption of Kaempferol molecules on the mild steel surface has been performed at molecular level by molecular dynamic simulations using Forcite quench molecular dynamics to sample different low energy configurations and identify the low energy minima. A careful observation of **Figure 17**, reveals that the Kaempferol molecule moved slowly ts near the Fe (110) surface and absorbed on the Fe (110) surface almost in parallel manner as the system reached equilibrium. The adsorption occurred through O-atom as well as -bond on the ring (Khaleed, 2010). Likewise, the binding energy ($E_{Binding}$) values between the metal surface and the inhibitor molecules are presented on Table 6. The potential energies were evaluated by taking the average energy of the lowest structure. The binding energy was negative showing stable adsorption structure. Also, the binding energy was <100 kcalmol , this is despite the fact that the simulations did not take into consideration the specific covalent interactions between the molecules and the Fe surface. The value was reported to be within the range of physisorption interactions (Li *et al.,* 2008; Shanableh, 2011; Singh, 2012; Yahaya *et al.,* 2012; Usman *et al,* 2014; Usman *et al.,* 2015; Bouayad *et al.,* 2018; Mohammed *et al.,* 2019; Ibrahim *et al*; 2020; Usman *et al.,* 2020; Bouklah *et al.*, 2020; El-Hassani *et al.,* 2020 Idris *et al.,* 2022; El Azzouzi, et al., 2022; Radi *et al.,* 2022; Ech -Chihbi, 2022).

Table 6: Binding Energies of the Adsorption of Kaempferol Molecule on the Fe (110) using Molecular Dynamic Simulation

Properties of Kaempferol Molecule	Values
Total P.E. (kcalmol^{-1})	-120.49
$E_{Inhibitor}$ (kcalmol^{-1})	-14.28
E_{Fe} (kcalmol^{-1})	-118.09
$E_{Interaction}$ (kcalmol^{-1})	-19.24
$E_{Binding}$ (kcalmol^{-1})	19.24

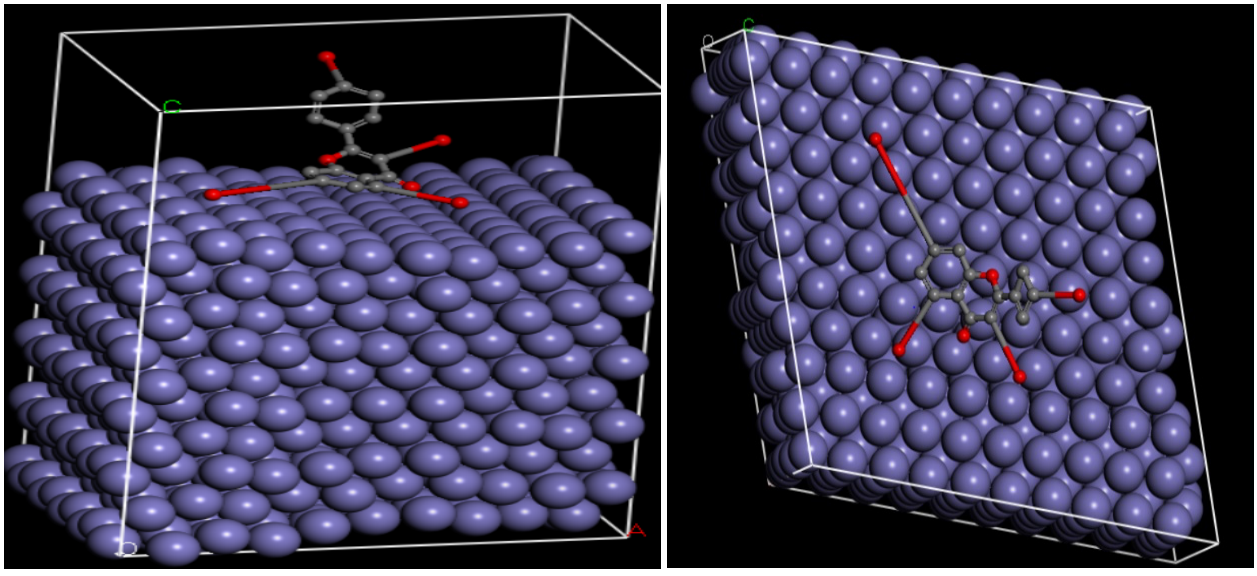

Side View of Kaempferol Molecule on the Mild Steel Surface Top View of Kaempferol Molecule on the Mild Steel Surface

Figure 17: Representation of the Inhibitor Iron Equilibrium Configuration

Conclusion

From the results it shows that SOL extract could be used as a promising corrosion inhibitor. Potantiodynamic polarization results evaluate SOL extract as cathodic type of inhibitor and the mechanism of the adsorptions on to the mild steel were explained clearly by EIS. The quantum chemical calculation and molecular dynamic simulation shows that, the result is consistent with the experimental

Acknowledgments: The authors acknowledge the funding by AMLAK Technology (Kaura, Zamfara State Nigeria) for their eminent support during this work as well as Petroleum Technology Development Fund (PTDF), Nigeria for giving scholarship is also acknowledged.

Disclosure statement: *Conflict of Interest:* The authors declare that there are no conflicts of interest.
Compliance with Ethical Standards: This article does not contain any studies involving human or animal subjects.

Reference

Abdallah M. (2004) Guar Gum as Corrosion Inhibitor for Carbon Steel in Sulphuric Acid Solutions, *Port. Electrochim* Acta. 22(4), 161-175.

Abiola K. O., Oforka N. C., Ebenso E. E., and Nwinuka N. M. (2007) Eco-friendly Corrosion Inhibitors: The Inhibitive Action of Delonix Regia Extract for the Corrosion Inhibition of Aluminium in Acidic Media. *Anti-Corros Method M.* 54(4), 219-224.doi.org/10.1108/00035590710762357

Abubakar M.S. and Usman B. (2019), Investigation of Corrosion Inhibition Potential of Ethanol Extract Balanites aegyptiaca Leaves on Mild Steel in 1M Hydrochloric Acid, *Mor. J. Chem.* 7 (1) 82-97, doi: .org/10.48317/IMIST.PRSM/morjchem-v7i1.14889

Alhassan Z., and Usman B. (2019) Optimization, Kinetic and Thermodynamic Studies of Mild steel Corrosion in different Soils. *Appl. J. Envir. Eng. Sci.* 5(3) 241-251, doi/org/10/48422/IMIST.

Asba A., Meeta B. (2017) Evaluation of Phytochemical of Cassia tora linn. And its Cytotoxicity Assay using Brine Shrimp. *International Journal of Pharmacognosy and Phytochemical Research*. (04), 587-595. doi.org/:10.25258/phyto.v9i2.8132

Bammou L., Mihit M., Salghi R., Bazzi L., Bouyanzer A., Al-Deyab S.S., Hammouti B. (2011) Inhibition Effect of Natural Artemisia Oils Towards Tinplate Corrosion in HCl solution: Chemical Characterization and Electrochemical Study, *Int. J. Electrochem. Sci.,* 6 N°5, 1454-1467.

Ben Hmamou D., Salghi R., Zarrouk A., Messali M., Zarrok H., Errami M., Hammouti B., Bazzi L. H., and Chakir A. (2012) Inhibition of steel corrosion in hydrochloric acid solution by chamomile extract, *Der Pharma Chim*. 4 (4), 1496-1505, doi.org.derpharmachemica.com/archive.html

Beniken M., Salim R., Ech-Chihbi E., Sfaira M., Hammouti B., Ebn Touhami M., Mohsin M. A., and Taleb M. (2022) Adsorption behavior and corrosion inhibition mechanism of a polyacrylamide on C–steel in 0.5 M H_2SO_4: Electrochemical assessments and molecular dynamic simulation, , *Journal of Molecular Liquids,* 348, 118022,doi.org/10.1016/j.molliq.2021.118022

Bishir U, (2015) Prediction of Corrosion Inhibition Efficiency of Thiophene Derivatives using Quantitative Structural Activity Relationship Method. An Unpublished PhD, Thesis, Department of Chemistry, Universiti Teknologi, Malaysia.

Bouayad K., Kandri Y., Elmsellen H., ElGhadraouni E., Ouzidan Y., Abde-Rahman I., Kusumu H.S., Warad I., Mague J. T., Essassi E.M., Hammouti B., and Chetouan A. (2018) Imidazo [4,5-b] pyridines as new class of corrosion inhibitor for mild. Experimental and DFT Approach, *Mor J. Chem. 6* (1) 22-34, doi.org/10.48317/IMIST.PRSM/morjchem-v6i1.9735

Boudalia M., Guenbour A., Bellaouchou A., Laqhaili A., Mousaddak M., Hakiki B., and Ebenso E.E. (2013) Corrosion Inhibition of Organic Oil Extract of Leaves of Lanvandula Stoekas on Stainless Steel in Concentrated Phosphoric Acid Solution. *Int. J. Electrochem Sci.* 8(4), 7414-7424

Bouklah M., Elmsellem H., Krim O., Serdaroğlu G., Hammouti B., Elidrissi A., Kaya S., and Warad I. (2020) Effect of substitution on corrosion inhibition properties of three Imidazole derivatives on mild steel in 1M HCl, Arab. *J. Chem. Environ. Res.* 07, 126-143, doi.org/10.1007/s12540-019-00381-5

Doughari J. H., El-Mahmood A. M., and Tyoyina I. (1998) Antimicrobial Activity of Leaves Extracts of Senna obtusifolia (L). *African Journal of Pharmacology.* 2(1), 007-013

Du L., Zhao H., Hu H., Zhang X., Ji L., Li H., Yang H., Li X., Shi S., Li R., Tang X., Yang J. (2014) Quantum Chemical and Molecular Dynamics Studies of Imidazole Derivatives as Corrosion Inhibitor and Quantitative Structure-Activity Relationship (QSAR) Analysis using the Support Vector Machine (SVM) Method. *Journal of Theoretical and Computational Chemistry.* 13(02), 22. doi.org/10.1142/S0219633614500126

Ebenso E. E., Eddy N. O, and Odiongenyi A.O. (2008) Corrosion Inhibitive Properties and Adsorption Behavior of Ethanol Extract of Piper guinensis as a Green Corrosion Inhibitor for Mild Steel in Sulphuric Acid. *African Journal of Pure ad Applied Chemistry* 2(11), 107-115

Ebenso E.E. (2003) Synergestic Effect of Halide Ions on Corrosion Inhibition of Aluminium in Sulphuric Acid using 2-acetylphenothiazine. *Journal of Materials Chemistry Physical.* 79(1), 58-70. doi.org/10.1016/S0254-0584(02)00446-7

Eddy N. O, and Odiongenyi A.O. (2010) Corrosion Inhibition and Adsorption Properties of Ethanol Extract of Heinsia crinata on Mild Steel in Sulphuric Acid. *Emrald Journal of Pigment and Resin Technology.* 39(5), 285-295. doi.org/ 10.1108/03699421011076407

Eddy N, and Ebenso. E.E. (2008) Adsorption and Inhibitive Properties of Ethanol Extracts of Musa sapientum peels as a Green Corrosion Inhibitor for Mild Steel in Sulphuric Acid. *African Journal of Pure and Applied Chemistry.* 2(6), 046-054

Eddy N.O. and Odoemelam S.A. (2009) Inhibition of the Corrosion of Mild Steel in Sulphuric Acid by Ethanol Extract of Aloe vera. *Pigment and Resin Technol,* 38(2), 111-115 doi.org/ 10.1108/03699420910940617.

El Azzouzi M., Azzaoui K., Warad K., Hammouti B., Shityakov S., Sabbahi R.S., Saoiabi S. M., Youssoufi M. H., Akartasse N., Jodeh S., Lamhamdi A., and Zarrouk A. (2022) Morrocon, Mauritania, and Senegalese gum Arabic variants as green corrosion inhibitors for mild steel in HCl: Weight loss, Electrochemical, AFM and XPS studies; *J. Mol. Liq.* 347, 118354, doi.org/10.1016/j.molliq.2021.118354 772

El Ghayati L., Batah A., Belkhouda M., Bammou L., Selghi R., Saber A., Chetouani A., Taha M. L., and Essassi E. M. (2019) Experimental and Theoretical investigation of 4-Methylene-2,3-dihydro-1H-1,5 benzodiazepin-one on the corrosion behavior steel in acidic media, *Mor. J. of Chem,* 7 (3), 567-57 doi.org/10.48317/IMIST.PRSM/morjchem-v7i3.17365

EL Hassani A. A., El Adnani Z., Benjelloun A. T., Sfaira M., Benzakour M., Mcharfi M., Hammouti B., and Emran K. M., (2020) DFT theoretical study of 5-(4-R-phenyl)-1H-tetrazole (R=H; OCH_3; CH_3; Cl) as corrosion inhibitors for mild steel in hydrochloric acid, *Met and Mater. Int.* 26(11) 1725–1733

Elmsellem H., Youssouf M. H., Aouniti A., Ben Hadda Chetouani A., and Hammouti B. (2014) Adsorption and inhibition effect of curcumin on mild steel corrosion in hydrochloric acid, *Russian J. Appl. Chem.*, 87 (6), 744-753 doi.org/10.1134/S1070427214060147

Ezeh E.M., Chinedu Agu P., (2023) Assessment of the Corrosion inhibitory potentials of *Chromolaena odorat* leaf extract on mild steel in hydrogen chloride acid environment, *Mor. J. Chem.,* 14(1), 188-204. https://doi.org/10.48317/IMIST.PRSM/morjchem-v10i3.30521

Ghazoui A., Benchat N., El-Hajjaji F., Taleb M., Rais Z., Saddik R., Elaatiaoui A., Hammouti B. (2017) The study of the effect of ethyl (6-methyl-3-oxopyridazin-2-yl) acetate on mild steel corrosion in 1M HCl, *Journal of Alloys and Compounds*, 693, 510-517, https://doi.org/10.1016/j.jallcom.2016.09.191

Husaini M., Ibrahim M. A., Ibrahim M.B., and Usman B. (2020) Effect of Aniline as Corrosion inhibitor on the Corrosion of Aluminium in Hydrochloric acid solution, *Research Journal of Chemistry and Environment,* 24(2), 99-106

Husaini M., Usman B., and Ibrahim M.B. (2019) Inhibtive Effect of Gluteraldehyde on the Corrosion of Aluminium in Hydrochloric Acid Solution. *Journal of Science and Technology*, 11(2), 8-16: doi.org/10.30880/jst.2019.11.02.002

Husaini M., Usman B., and Ibrahim M.B. (2019) Study of Corrosion Inhibition of Aluminium in Nitric Acid solution using Anisaldehyde (4-Methoxy Benzaldehyde) as corrosion Inhibitor, *Algerian Journal of Engineering and Technology*, 1, 11-.doi.org/10.5281/zenodo.3477599

Ibrahim M.B., Sulaiman Z., Usman B., and Muhammad A. I. (2019) Effect of Henna Leaves on the Corrosion inhibition of Tin in Acidic and Alkaline Medium, *World Journal of Applied Chemistry* 4(4) 54-51, doi.org/10.11648/j.wjac.20190404.11

Idris I. A., Bello A. U., and. Usman B. (2022) Experimental and Theoretical evaluation of corrosion inhibition of honey comb propolis extract On Mild Steel in Acid media. *J. Mater. Environ. Sci.* 13 (5) 576-598

Jain S., and Patil U. K. (2010) Phytochemical and Pharmacological Profile of Cassia tora linn. *Indian Journal of Natural Products and Resources.* 1(4)430-437.

Jimoh I. and Usman B. (2021) Corrosion Inhibition Effect of Ethanol Extract of Acacia nilotica Leaves on Mild Steel in Acid Medium. *Port. Electrochim Acta,* 39 ,105-128, doi.org/10.4152/pea.202102105

Kadhim A. S. (2016). Inhibition of Aluminium (AA3105) Corrosion in HCl by Acetamide and Thiourea. *Nigerian Journal of Corrosion.* 17(10) 441-452.

Kahled F. K. (2010), Studies of Iron Corrosion Inhibition using Chemical, Electrochemical and Computer Simulation Techniques. *Electrochimica Acta.* 55(22), 6523-6532. doi.org/10.1016/j.electacta.2010.06.027

Kalaichelvi K. and Dhivya S.M. (20017), Screening of Phytoconstituents, UV-Vis Spectrum and FTIR Analysis of Micrococca marcurials (L.) Benth. *Int. J. Herb.* 5(6) 40-44.

Li W., He Q., Zheng S., Pei C., and Hou B., (2008) Some New Triazole Derivatives as Inhibitors for Mild Steel by Acidic Extracts. *J. Appl Electrochem.* 38. 289-295. doi.org/10.1007/s10800-007-9437-7

Mohamed K. A. (2019) Quantum Chemical Studies and Molecular Modelling of the Effect of Polyethylene Glycol as Corrosion Inhibitors of an Aluminium Surface. *Can. Journal of Chemistry.* 91 (2019) 283-291.doi.org/10.1139/cjc-2012-0354

Murulana L.U. (2015) Adsorption, Thermodynamic, and Density Functional Theory Investigation of some Sulphonamides as Corrosion Inhibitors for some selected Mild Steel in Acidic Medium. An Unpublished PhD. Thesis Submitted to the Department of Chemistry, Faculty of Agric. Science and Technology, North-west University,

Obot I. B., Umoren S. A., and Ebenso E.E. (2011) Computational Simulation and Statistical Analysis on the Relationship between Corrosion Inhibition Efficiency and Molecular Structure of some Phenanthroline Derivatives on Mild Steel Surface. *Int. J. Electrochem. Sci.* 6(2), 5649-5675.

Omotosho A.O. (2016) Inhibition Evaluation of Chemical and Plant Extracts on the Corrosion of Metallic Alloys in Acidic Environment. An Unpublished PhD. Thesis, Covenant University of Nigeria.

Onen I. A. (2010) Kinetic Studies of Selected Corrosion Inhibitors of Aluminium in Mild Steel in Acidic Medium. An Unpublished PhD. Thesis Submitted to the Dept. of Chemisty, Natural Science, University of Jos, Nigeria.

Popoola A.P.I., Sanni O., Lotoa C.A., and Popoola O. M. (2015) Corrosion Inhibition: Synergistic Influence of Gluconates on Mild Steel in Different Corrosive Environments. Synergetic Interaction of Corrosion Inhibition Tendency of Two Different Gluconates on Mild Steel in Different Environments. *Port. Electrochim Acta.* 33(6) 353-370. doi.org/10.4152/pea.201506353

Prakash J., Singh H., Khan G., and Baccha U. (2015) Application of Aqueous Extracts of Coffee senna for Control of Mild Steel Corrosion in Acidic Environments. *Int. J. Ind. Chem.* 3(13) (2015) 481-489. doi:10.1186/2228-5547-3-13

Radi A., El Mahi B., Aouniti A., El Massoudi M., Radi S., Kaddouri M., Chelfi T., Jmiai A., El Asri A., Hammouti B., Warad I., Guenbour A. and Zarrouk A. (2022) Mitigation effect of novel bipyrazole ligand and its copper complex on the corrosion behavior of steel in HCl: Combined experimental and computational studies, *Chem. Phys Lett,* 795, 139532, doi.org/10.1016/j.cplett.2022.139532

Shanableh A. (2011) Studies on Natural Extracts as Inhibitors for Mild Steel Corrosion in 1M HCl Solution. An Unpublished PhD. Thesis Submitted to the Dept. of Chemical Eng. Faculty of the American University of Sharjah College of Engineering..

Singh. A.K. (2012), Inhibition of Mild Steel Corrosion in HCl Solution by 3-(4-(z)-indolin-3-ylideneamino) indolin-2-one. *Industrial and Eng. Chem. Res*. 51, 3215-3223. doi.org/10.1021/ie2020476

Umar B. A, Uzairu A and Shallangwa.G.A. (2019), Understanding Inhibition of Steel Corrosion by Some Potent Triazole Derivatives of Pyridine through Density Functional Theory and Molecular Dynamics Simulation Studies. *J. Turkish. Chem. Soc.* 6(03), 451-462. doi.org/10.18596/jotcsa.446084

Umoren S. A., Obi-Egbedi N. O., and Obot. I. B. (2012) Spondias mombin L. as a Green Corrosion Inhibitor for Aluminium in Sulphuric Acid: Correlation between Inhibitive Effect and Electronic Properties of Extracts Major Constituents using Density Functional Theory. A*rab. J. Chem.* 5(3), 361-373. doi.org/10.1016/j.arabjc.2010.09.002

Usman A., Farouk H. U., and Usman B. (2020) Inhibition performance of camel dung extract on the corrosion of Mild Steel in hydrochloric acid, *Alg. J. Mat. Chem.* 3 (2), 77-89, doi.org/10.5281/zenodo.4488687

Usman B., Hasmerya M., Abdallah H. H., and Aziz M. (2015) Computational Evaluation of the Effect of Structural Parameters of 3-Fluoro Thiophene and 3-Thiophene Malonic Acid on Corrosion Inhibition Efficiency of Mild Steel in Acid Media. *Int. J. Electrochem.* Sci. 10, 3223-3229.

Usman B., Maarof H., Abdallah H. H., Jamaludin R., Hasan M, N., and Aziz M. (2014) Theoretical and Experimental Studies of Corrosion Inhibition of Thiophene-2-Ethylamine on Mild steel in Acidic Media. *J.Teknol(Science and Engineering)*76(13), 7-14, doi.org/10.11113/jt.v76.5813

Usman B., Maaroof H., Abdallah H. H., Jamaludin R., Al-fakih A., and Aziz M. (2014) Corrosion Inhibition Efficiency of Thiophene Derivatives on Mild Steel: A QSAR Model. *Int. J. Electrochem.* Sci. 9, 1678-1689.

Usman B., Umar A. B., and Mohammed A. S. (2018) Quantum Chemical Evaluation on Corrosion Inhibition Performance of Belanitin-7 on Mild Steel in 1M HCl Acid Solution. *Appl. J. Envir. Eng. Sci.,* 4(3), 380-386.

Yahaya H., Olaeshinde E. F., Olesegun S. J., Adesina A. S., and Omogbehin S.A. (2012) Inhibitory Action of Nicotania tabacum Extracts on the Corrosion of Mild Steel in HCl: Adsorption and Thermodynamic Study. *Nat. Sci.* 10(12) 21-34

Zerga B., Sfaira M., Rais Z., Ebn Touhami M., Taleb M., Hammouti B., Imelouane B., Elbachiri A. (2009) Lavender oil as an ecofrindly inhibitor for mild steel in 1 M HCl, Materiaux et Technique, 97 N°5, 297-305

(2023) ; https://revues.imist.ma/index.php/morjchem/index